Hindawi
Journal of Nanomaterials
Volume 2018, Article ID 7049675, 8 pages
https://doi.org/10.1155/2018/7049675

Research Article

Rhodamine Derivative Functionalized Magnetic Nanoplatform for Cu^{2+} Sensing and Removal

Jiaxin Wang,[1] Shuhan Wang,[1] Wanqing Tian,[2] Dong Yao,[2] Lining Sun,[1] Liyi Shi,[1] and Jinliang Liu[1]

[1]*Research Center of Nano Science and Technology, Shanghai University, Shanghai 200444, China*
[2]*Jingjiang Hospital of Traditional Chinese Medicine, Jiangsu Province 214500, China*

Correspondence should be addressed to Jinliang Liu; liujl@shu.edu.cn

Received 29 March 2018; Accepted 6 May 2018; Published 10 June 2018

Academic Editor: Xuping Sun

Copyright © 2018 Jiaxin Wang et al. This is an open access article distributed under the Creative Commons Attribution License, which permits unrestricted use, distribution, and reproduction in any medium, provided the original work is properly cited.

Pollution caused by copper is one of the key factors of environment contamination. As one of the heavy metals, copper is hard to decompose in nature; the biological enrichment of which may lead to severe damage to health. Cu^{2+} detection, thus, possesses a bright application prospect both in environment protection and in human health. In this paper, a dual-functional fluorescence-magnetic composite nanoplatform has been designed to sensitively detect, meanwhile, capture, and remove Cu^{2+} in the solution of water and ethanol (1 : 1, *v*/*v*). The core-shell structure nanoparticle synthesized by using Fe_3O_4 as core and SiO_2 as shell is covalently bonded with rhodamine derivatives on the silica layer to construct the nanoplatform. The emission is increased upon the addition of Cu^{2+}, showing fluorescence turn on effect for the detection, and the limit of detection is as low as 1.68 nM. Meanwhile, Cu^{2+} ions are captured by the coordination with rhodamine derivatives and can be removed with the help of magnetic field.

1. Introduction

With the increasing development of social productivity, copper pollution as a representative of heavy metal contamination is getting worse. Copper dust, which is made by the weathering of the rocks, mining, metallurgy, and machine process, will result in pollution of air, water, and soil [1–3]. Meanwhile, copper is hard to decompose in nature, and the resulting enrichment through food chain may lead to severe damage to health [4, 5]. As an essential trace element, copper ions, if in improper dose [6], are likely to cause human poisoning, and illness involves the nervous system, digestive system, cardiovascular system, endocrine system, and so on, among which are known to the majority including Alzheimer's disease, hepatic cirrhosis, leucoderma, and skeleton deformity [7–10]. Therefore, the development of new methods for the detection and removal of copper ions in the environment has attracted a lot of research interests in the past decades.

There are many techniques at present to detect Cu^{2+}, such as atomic absorption spectrometry (AAS), inductively coupled plasma atomic emission spectrometry (ICP-AES), and inductively coupled plasma mass spectrometry (ICP-MS) [11–13]. But difficulties still exist in trace analysis, due to the limited sensitivity and detection limits (LOD) of machine. In addition, expensive test cost, large amounts of time in sample preparation, and inconvenience for on-site analysis are the stumbling blocks to Cu^{2+} detection, both in life and environment. As an effective approach, the florescence method has advantages of technical simplicity, high sensitivity, fast response time, and nondestructive imaging [14–16]. In terms of florescence determination, the key procedure is to design and synthesize fluorescent probes to detect metal ions or biomolecules by monitoring luminescence quenching [17–20] or enhancement phenomenon [21–23] upon the interaction with testing samples. Lots of fluorescent probes have been developed for detection of Cu^{2+} ions with high sensitivity and selectivity [24–26].

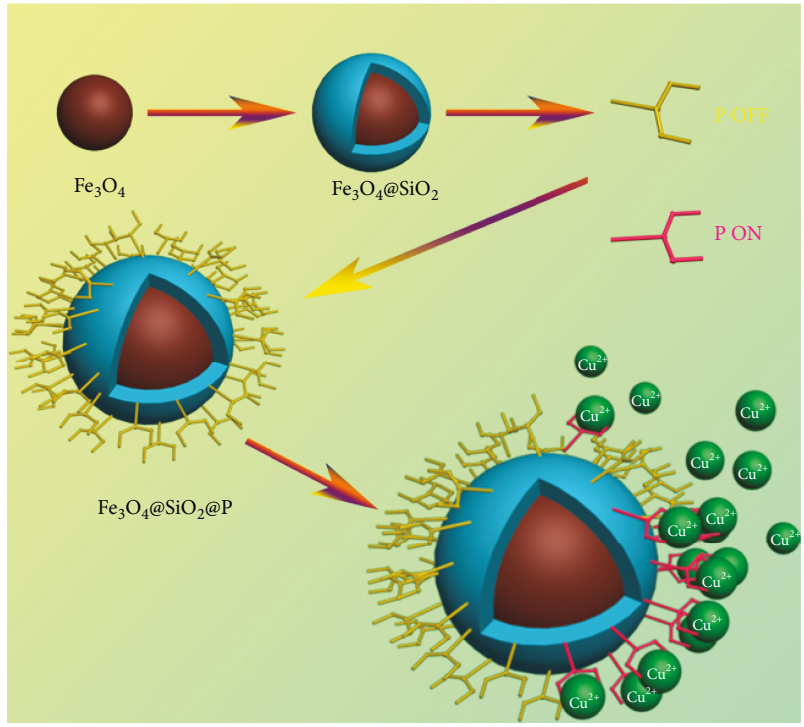

Scheme 1: Schematic illustration of the synthetic procedure of the $Fe_3O_4@SiO_2@P$ and the proposed sensing and removal mechanism of $Fe_3O_4@SiO_2@P$ towards Cu^{2+} ions.

Among these reports, rhodamine compounds have shown significant advantages over some traditional fluorophores due to their attractive feature such as high photostability, wide wavelength range, and high fluorescence quantum yield and thus become an extensive research topic in the field of chemistry and biology [27–30]. However, fluorescent probes with single structure often suffer from some drawbacks, such as low detect efficiencies, separation difficulties, and secondary pollution to environment. Nanoplatform which combined the inorganic-organic composite together fills the gap by its prominent advantages in complementation and cooperatives in multifunction. As for inorganic composite, magnetic nanoparticles provide us an environmental friendly way of separation and recycle [31–33]. There are different ways in ion detection and removal based on the functionalized magnetic nanoplatform. One of the common ways is adsorption. For instance, Cu^{2+} ions are absorbed by hydroxyl groups from β-cyclodextrin and silane [34]. Another method of ion capture is coordination; for example, 8-hydroxyquinoline-2-carboxylic acid is adopted as chelator to coordinate with copper ions [35].

As one of the famous fluorescent probes, rhodamine derivatives have advantages on high absorbance, improved fluorescence quantum yield, and better photostability. Superparamagnetic nanomaterial is suitable for magnetic separation and fast enrichment. In this work, we have designed a core-shell-structured nanoplatform, in which Fe_3O_4 is core, SiO_2 is shell, and rhodamine derivatives are loaded on the layer of SiO_2. The synthesized hybrid can realize the fluorescence turn on effect for the Cu^{2+} detection and Cu^{2+} removal with the help of external magnetic field.

2. Experimental Section

2.1. Materials. 1-Octadecene (ODE, technical grade, 90%), oleic acid (OA, technical grade, 90%), IGEPAL CO-520, and tetraethyl orthosilicate (TEOS, GC, ≥99%) were purchased from Sigma-Aldrich Co. Ltd. (China). Sodium oleate (CP), n-Hexane (AR, 97%), ammonia solution (AR), and salicylaldehyde were obtained from Shanghai Aladdin Chemistry Co. Ltd. (Shanghai, China). Hydrazine hydrate (85%), rhodamine B, and (3-isocyanatopropyl)triethoxysilane (GR, 95%) were purchased from J&K Technology Co. Ltd. Toluene (AR), iron (III) chloride hexahydrate (AR), and anhydrous ethanol (99.7%, AR) were obtained from Sinopharm Chemical Reagent Co., China. All the agents above were used without further purification. Aqueous solution of different ions, such as Cu^{2+}, K^+, Ba^{2+}, Co^{2+}, Ca^{2+}, Na^+, Mn^{2+}, Mg^{2+}, Ni^{2+}, and Hg^+, was prepared, respectively, from its chloride salts. Water used during the experiments was deionized water.

2.2. Preparation of $Fe_3O_4@SiO_2$. Fe_3O_4 was synthesized through pyrolysis method according to the previous report [36] with some modification. 40 mmol of $FeCl_3{\cdot}6H_2O$ and 40 mmol of sodium oleate were dispersed into 80 mL of ethanol. Then, the resulted solution was mixed with 60 mL of deionized water and 140 mL of n-hexane and kept in 70°C for 4 h. After that, 30 mL of deionized water was then added to wash the product. At last, the oil phase was gathered and dried overnight. Next, 36 g of the resulting iron oleat complex was dissolved in 20 mmol of OA and 200 g of ODE; the mixture was reacted at 320°C for 30 min under Ar. After cooling at room temperature, the solid product was

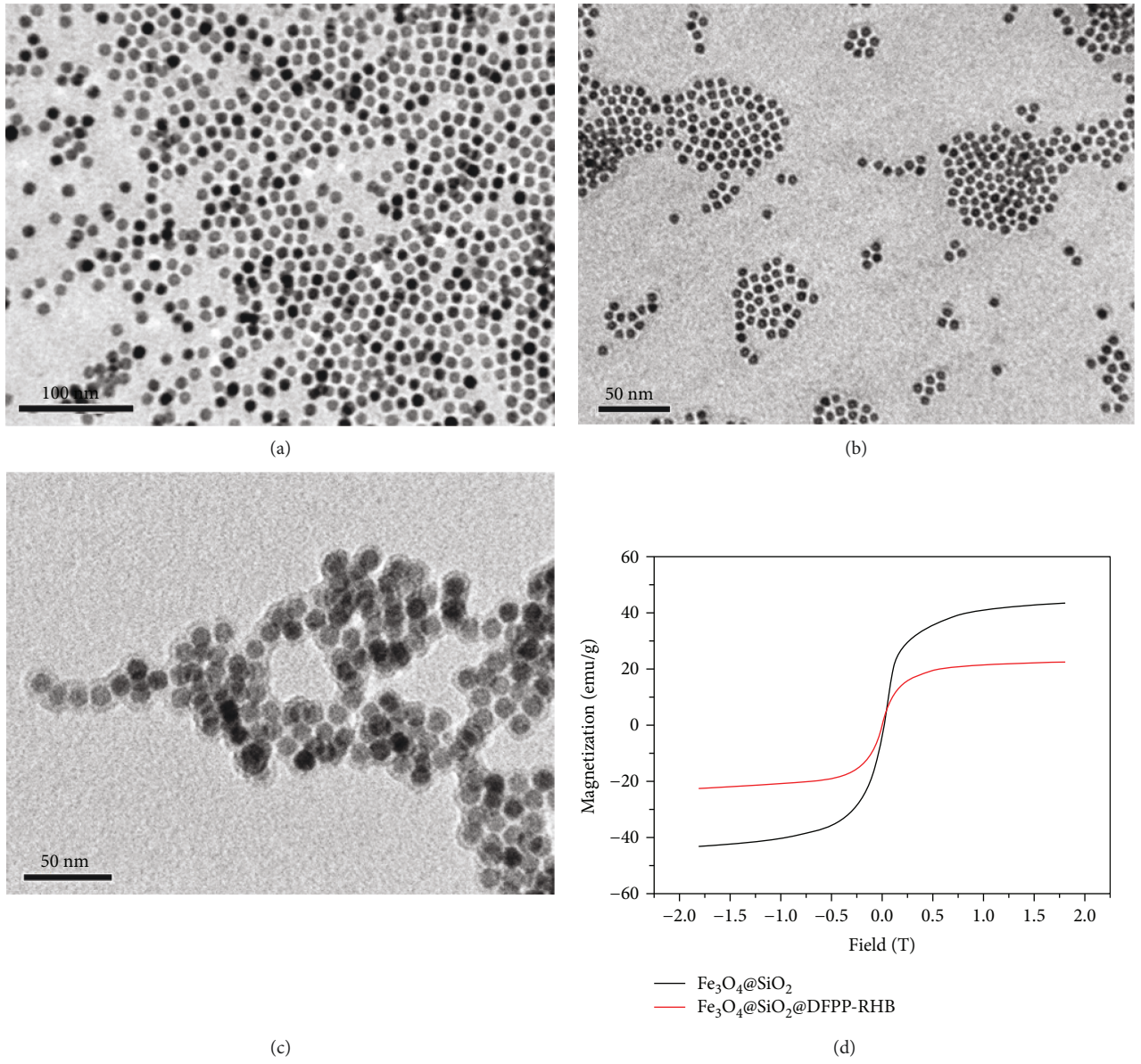

Figure 1: The TEM images of (a) Fe_3O_4, (b) Fe_3O_4@SiO_2, and (c) Fe_3O_4@SiO_2@P. (d) Magnetic hysteresis loop of Fe_3O_4@SiO_2 (black line) and Fe_3O_4@SiO_2@P (red line).

collected and washed with 20 mL of n-hexane for 3 times. Finally, the nanocrystals were dispersed in n-hexane (30 mg/mL) for storage.

Reversed-phase microemulsion method was used in forming silica layer outside of the Fe_3O_4. 250 μL of Fe_3O_4 dispersion was diluted with 10 mL of n-hexane. 50 μL of CO-520 was added while vigorously stirring, then kept at the same condition continuously for 30 min. Next, 2 μL of TEOS was added slowly. Afterwards, 10 μL of ammonia solution was added and the mixture was stirred continuously for 20 h. The resulting products were washed using ethanol as precipitant via centrifugal separation for 3 times. At last, Fe_3O_4@SiO_2 was obtained and dispersed in 5 mL of ethanol at 4°C.

2.3. Preparation of Fe_3O_4@SiO_2@P. The rhodamine derivative (P for short) was synthesized according to our previous article [37]. 60 mg of Fe_3O_4@SiO_2 nanoparticles was redispersed in 20 mL of toluene, and then the solution was heated to 80°C. 20 μL of (3-isocyanatopropyl)triethoxysilane was added by drops, and the temperature was kept at 110°C for 12 h. After that, P (120 mg) distributed in 1 mL of toluene was injected into the reactant rapidly and then, kept at 110°C for another 12 h. After cooling down to room temperature, Fe_3O_4@SiO_2@P was collected via centrifugation and washed with alcohol for three times. Finally, Fe_3O_4@SiO_2@P was dispersed in 5 mL of ethanol and sealed for storage at 4°C for further use.

2.4. Characterization. The morphology features of nanoparticles were observed by transmission electron microscope (TEM, JEM-200CX) at 200 kV. Vibrating sample magnetometer (VSM, 7407; lakeshore) was used for evaluating the

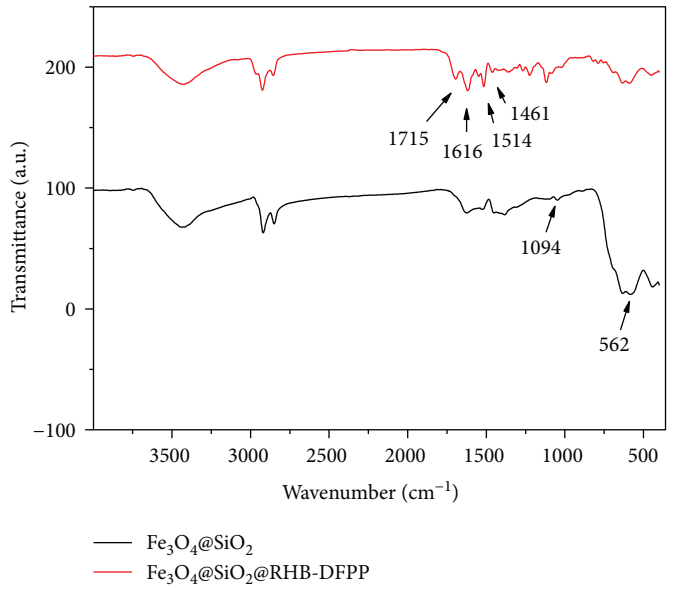

Figure 2: FTIR spectra of Fe_3O_4@SiO_2 and Fe_3O_4@SiO_2@P.

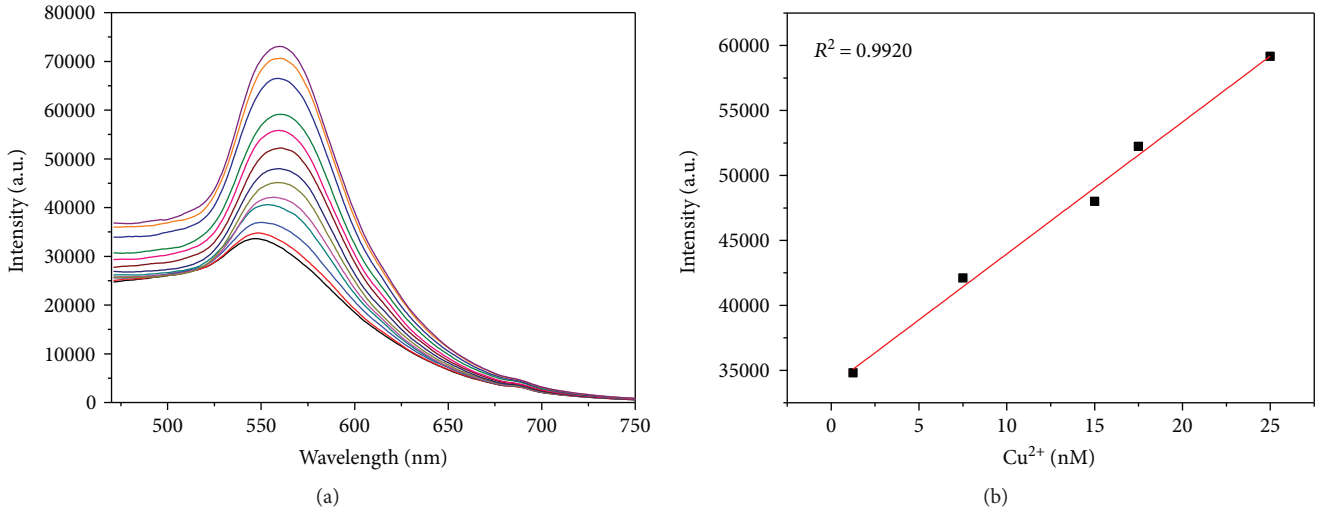

Figure 3: The emission spectra (a) of Fe_3O_4@SiO_2@P upon various concentrations of Cu^{2+} (λ_{ex} = 520 nm); the linear fitting of florescence intensities at peak of 550 nm towards the concentrations of Fe_3O_4@SiO_2@P (b).

magnetic properties at room temperature. Fourier transform infrared (FTIR, AVATAR370, Nicolet) spectroscopy was to analyze functional groups from synthesized materials. Structure analysis of organic molecules was performed by Fourier superconducting nuclear magnetic resonance spectrometer (AVANCE 500 MHz, BRUKER), using tetramethylsilane (TMS) as an internal standard. To detect the actual ion concentrations, inductively coupled plasma atomic emission spectroscopy (ICP-AES, HORIBA JOBIN YVONSAS) was employed. Fluorescent properties were determined by a LS-55 spectrophotometer. The excitation wavelength was 520 nm, and the emissions were collected from 470 to 750 nm. All the measurements mentioned above were conducted at room temperature.

2.5. Cu^{2+} Response and Removal. A stock solution of Fe_3O_4@SiO_2@P (10 mg/mL) was prepared in the solution of water and ethanol (1 : 1, *v*/*v*). Stock solutions of the metal ions (0.1 M) were prepared in deionized water. Titration experiments were performed by adding Cu^{2+} solution incrementally to a solution of Fe_3O_4@SiO_2@P (2.5 mL). For the selectivity experiments, the test samples were prepared by adding appropriate amounts (100 equiv.) of metal ion solution to 2.5 mL of a solution of Fe_3O_4@SiO_2@P. In competition experiments, Cu^{2+} was added to the solutions containing Fe_3O_4@SiO_2@P and other metal ions of interest. In Cu^{2+} removal experiments (three parallels), Cu^{2+} (1 mL, 0.1 M) was added in Fe_3O_4@SiO_2@P (2.5 mL) and dispersed evenly. Under magnet treatment, the resulted supernate was

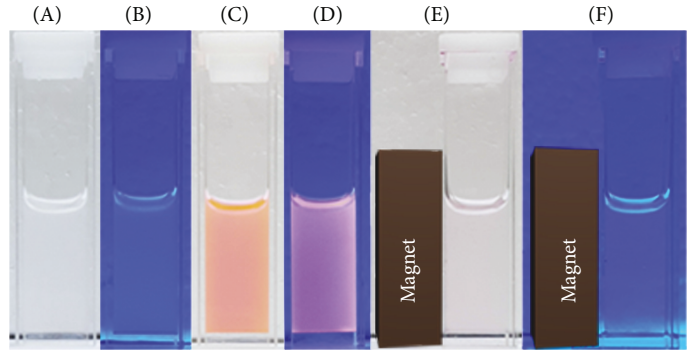

(a)

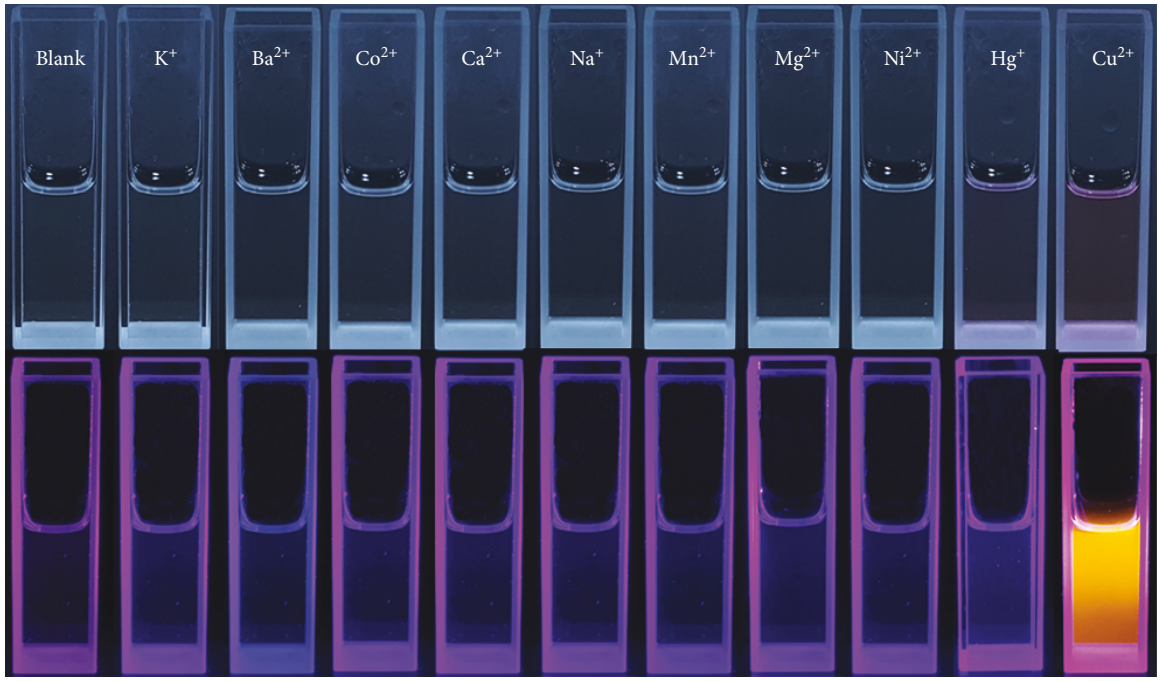

(b)

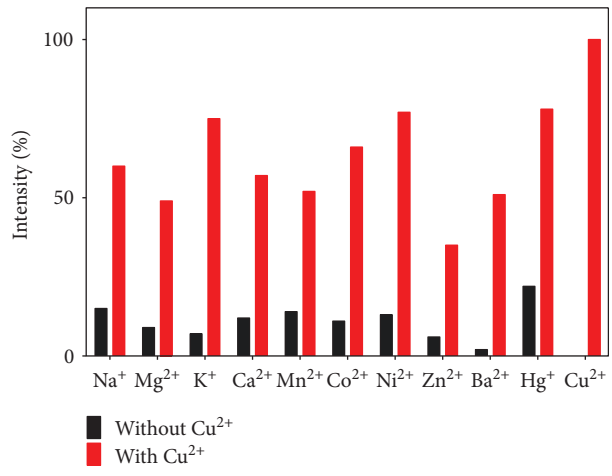

(c)

Figure 4: (a) Photos of Fe_3O_4@SiO_2@P with (C–F) or without (A, B) Cu^{2+} under daylight (A, C, E) or UV-visible light (B, D, F) by using magnet (E, F) or no magnet (A–D); (b) photos of Fe_3O_4@SiO_2@P after the addition with various metal ions, respectively; (c) ion competition experiment of Fe_3O_4@SiO_2@P in the presence of 2.5 μM Cu^{2+}, upon the background of various metal ions (2.5 μM).

collected, respectively, after 5 min and 10 min. All solutions were stirred for 3 min at room temperature and then used for the spectroscopic test.

3. Results and Discussions

3.1. Morphology and Structure Characterization. As illustrated in Scheme 1, Fe_3O_4 nanoparticle was designed as the core, and its intrinsic magnetism was the critical factor for separation and removal of Cu^{2+} with external magnetic field. As Figure 1(a) showed, Fe_3O_4 was uniform and monodisperse and the measured diameter was 9.88 ± 0.79 nm. By utilizing reversed-phase microemulsion method, solid silica was coated on the surface of Fe_3O_4 via hydrolysis-condensation reaction of TEOS. The obtained $Fe_3O_4@SiO_2$ possessed regular morphology with the average diameter of 21.63 ± 1.57 nm, and the average thickness of silica layer was about 5 nm measured from the TEM images (Figure 1(b)). The magnetic nanoplatform $Fe_3O_4@SiO_2@P$ was finally achieved by the nucleophilic addition reaction between the amino group of (3-isocyanatopropyl)triethoxysilane and the hydroxyl group of P. Some aggregation appeared after loading of P (Figure 1(c)); this is mainly because of the hydrophobic property of the organic probe molecule P. The saturated magnetization of $Fe_3O_4@SiO_2$ was 43.4 emu/g, as shown in Figure 1(d). After combining with organic probe molecules, the saturated magnetization of the hybrid probe was decreased to 22.6 emu/g. It is suggested that the outer nonmagnetic composite leads to the decrease of maximum saturation magnetizations.

Fourier transform infrared spectroscopy (FTIR) of $Fe_3O_4@SiO_2$ and $Fe_3O_4@SiO_2@P$ was carried out in order to testify the successful loading of P. As Figure 2 showed, FTIR of $Fe_3O_4@SiO_2$ exhibited two characteristic bands of silica layer. Peak at 1094 cm^{-1} was attributed to Si-O-Si symmetric stretching vibrations, and peak at 562 cm^{-1} was assigned to Si-O symmetric stretching vibrations. The spectrum of $Fe_3O_4@SiO_2@P$ showed C=C symmetric stretching vibrations at 1616 cm^{-1}, 1514 cm^{-1}, and 1461 cm^{-1}, which belonged to benzene ring. Also, C=O stretching vibration at 1715 cm^{-1} was appeared; thus, it could be concluded that covalent bonding existed between P and silica.

3.1.1. Sensing and Capture of Cu^{2+}. The ion-responsive mechanism was achieved due to the well-known equilibrium between the nonfluorescent spirolactam and the fluorescent ring-opened amide of rhodamine. The emission spectrum of $Fe_3O_4@SiO_2@P$ upon various concentrations of Cu^{2+} is shown in Figure 3(a). Under the excitation at 520 nm, the emission bands centered at 552 nm appear and the intensities increase evidently with the Cu^{2+} concentration increased. This indicates that the ring-open process of the rhodamine B unit in P happened. A linear correlation between the emission intensity and concentration of Cu^{2+} in the range of 0–25 nM can be observed (Figure 3(b)). The limit of detection (LOD) was calculated as low as 1.68 nM by the following formula $LOD = 3S_0/S$ (where S_0 is the standard deviation of the blank measurements, S is the slope of the calibration curve, and 3 is the factor at the 99% confidence level), suggesting the high sensitivity of the nanoplatform for detecting Cu^{2+}.

Benefits from the intrinsic structure of P and the magnetic properties of Fe_3O_4, the nanoplatform can realize the fluorescent detection of Cu^{2+} with naked eyes and removal of Cu^{2+} with the help of magnetic field. As shown in Figure 4(a), before the addition of Cu^{2+}, the hybrid nanoplatform was light brown color and nonflorescent. When Cu^{2+} was added, the hydrazide group and O-acyl hydroxylamines bonded with Cu^{2+}, and thus led to the opening of the spirolactam ring in P molecule. The resulting conjugate π-bond facilitates the enhancement of florescence intensity at 550 nm. Also, photoinduced electron transfer (PET) was blocked; thus, the solution of fluorescence probe turned into pink color [38–40]. The Cu^{2+} removal effect of the nanoplatform was shown in Figure 4(a) (E, F). We can see that, after a few seconds, the nanoplatform together with Cu^{2+} gathered to the side of cuvette under magnetic felid treatment. The removal efficiency of Cu^{2+} was 75% calculated from ICP-AES results. Furthermore, the selective experiments were done to demonstrate the nanoplatform which can detect Cu^{2+} exclusively over other metal ions. As shown in Figure 4(b), there was nearly no color change upon the introduction of other metal ions, including K^+, Ba^{2+}, Co^{2+}, Ca^{2+}, Na^+, Mn^{2+}, Mg^{2+}, Ni^{2+}, and Hg^{2+}. Additionally, competition experiments were further carried out by adding Cu^{2+} to the solutions containing both nanoplatform and the metal ions of interest. As shown in Figure 4(c), these coexistent ions had negligible interference on Cu^{2+} sensing; even the competitive ions were present at high concentrations.

4. Conclusions

In brief, a dual-functional hybrid nanoplatform $Fe_3O_4@SiO_2@P$ had been successfully prepared. In this nanoplatform, the Fe_3O_4 as the core endowes it with magnetism; SiO_2 as one thin layer bridges the inorganic-organic composites together; rhodamine derivative P is designed for fluorescent sensing of Cu^{2+}. Benefits from the intrinsic structure of P and the magnetic properties of Fe_3O_4, the nanoplatform can realize the fluorescent detection of Cu^{2+} with naked eyes and removal of Cu^{2+} with the help of magnetic field. This nanoplatform was featured on simple operation, uniform particle size, structural stability, and excellent magnetic responsibility and thus can be used for the cell imaging of Cu^{2+} or removal of Cu^{2+} from the environmental pollution.

Data Availability

The data used to support the findings of this study are available from the corresponding author upon request.

Conflicts of Interest

The authors declare that they have no conflicts of interest.

Acknowledgments

The authors are grateful for the financial support from the National Natural Science Foundation of China (Grant nos. 21201117 and 21231004) and Medical Research Project of Jiangsu Provincial Commission of Health and Family Planning (no. Z201624).

References

[1] S. Dragovic and N. Mihailovic, "Analysis of mosses and topsoils for detecting sources of heavy metal pollution: multivariate and enrichment factor analysis," *Environmental Monitoring and Assessment*, vol. 157, no. 1–4, pp. 383–390, 2009.

[2] M. Huber, A. Welker, and B. Helmreich, "Critical review of heavy metal pollution of traffic area runoff: occurrence, influencing factors, and partitioning," *Science of the Total Environment*, vol. 541, pp. 895–919, 2016.

[3] Q. Ding, G. Cheng, Y. Wang, and D. F. Zhuang, "Effects of natural factors on the spatial distribution of heavy metals in soils surrounding mining regions," *Science of the Total Environment*, vol. 578, pp. 577–585, 2017.

[4] D. V. Nesterkova, E. L. Vorobeichik, and I. S. Reznichenko, "The effect of heavy metals on the soil-earthworm-European mole food chain under the conditions of environmental pollution caused by the emissions of a copper smelting plant," *Contemporary Problems of Ecology*, vol. 7, no. 5, pp. 587–596, 2014.

[5] R. Dallinger and W. Wieser, "The flow of copper through a terrestrial food chain," *Oecologia*, vol. 30, no. 3, pp. 253–264, 1977.

[6] J. R. Prohaska, "Impact of copper deficiency in humans," *Annals of the New York Academy of Sciences*, vol. 1314, no. 1, pp. 1–5, 2014.

[7] K. Jomova, S. Baros, and M. Valko, "Redox active metal-induced oxidative stress in biological systems," *Transition Metal Chemistry*, vol. 37, no. 2, pp. 127–134, 2012.

[8] N. F. Suttle, "Copper imbalances in ruminants and humans: unexpected common ground," *Advances in Nutrition*, vol. 3, no. 5, pp. 666–674, 2012.

[9] K. Y. Djoko, B. M. Paterson, P. S. Donnelly, and A. G. McEwan, "Antimicrobial effects of copper(II) bis(thiosemicarbazonato) complexes provide new insight into their biochemical mode of action," *Metallomics*, vol. 6, no. 4, pp. 854–863, 2014.

[10] C. Wijmenga and L. W. J. Klomp, "Molecular regulation of copper excretion in the liver," *Proceedings of the Nutrition Society*, vol. 63, no. 1, pp. 31–39, 2004.

[11] A. Zhuravlev, A. Zacharia, M. Arabadzhi, C. Turetta, G. Cozzi, and C. Barbante, "Comparison of analytical methods: ICP-QMS, ICP-SFMS and FF-ET-AAS for the determination of V, Mn, Ni, Cu, As, Sr, Mo, Cd and Pb in ground natural waters," *International Journal of Environmental Analytical Chemistry*, vol. 96, no. 4, pp. 332–352, 2016.

[12] Y. G. Tu, Y. Zhao, M. S. Xu, X. Li, and H. Y. Du, "Simultaneous determination of 20 inorganic elements in preserved egg prepared with different metal ions by ICP-AES," *Food Analytical Methods*, vol. 6, no. 2, pp. 667–676, 2013.

[13] Z. H. Li, J. X. Chen, M. S. Liu, and Y. L. Yang, "Supramolecular solvent-based microextraction of copper and lead in water samples prior to reacting with synthesized Schiff base by flame atomic absorption spectrometry determination," *Analytical Methods*, vol. 6, no. 7, pp. 2294–2298, 2014.

[14] Y. Zhou, Z. Xu, and J. Yoon, "Fluorescent and colorimetric chemosensors for detection of nucleotides, FAD and NADH: highlighted research during 2004–2010," *Chemical Society Reviews*, vol. 40, no. 5, pp. 2222–2235, 2011.

[15] H. N. Kim, Z. Q. Guo, W. H. Zhu, J. Yoon, and H. Tian, "Recent progress on polymer-based fluorescent and colorimetric chemosensors," *Chemical Society Reviews*, vol. 40, no. 1, pp. 79–93, 2011.

[16] H. N. Kim, W. X. Ren, J. S. Kim, and J. Yoon, "Fluorescent and colorimetric sensors for detection of lead, cadmium, and mercury ions," *Chemical Society Reviews*, vol. 41, no. 8, pp. 3210–3244, 2012.

[17] L. Yang, D. N. Liu, S. Hao et al., "Topotactic conversion of α-Fe_2O_3 nanowires into FeP as a superior fluorosensor for nucleic acid detection: insights from experiment and theory," *Analytical Chemistry*, vol. 89, no. 4, pp. 2191–2195, 2017.

[18] J. Q. Tian, N. Y. Cheng, Q. Liu, W. Xing, and X. P. Sun, "Cobalt phosphide nanowires: efficient nanostructures for fluorescence sensing of biomolecules and photocatalytic evolution of dihydrogen from water under visible light," *Angewandte Chemie International Edition*, vol. 54, no. 18, pp. 5493–5497, 2015.

[19] W. B. Lu, X. Y. Qin, S. Liu et al., "Economical, green synthesis of fluorescent carbon nanoparticles and their use as probes for sensitive and selective detection of mercury(II) ions," *Analytical Chemistry*, vol. 84, no. 12, pp. 5351–5357, 2012.

[20] S. Liu, J. Q. Tian, L. Wang et al., "Hydrothermal treatment of grass: a low-cost, green route to nitrogen-doped, carbon-rich, photoluminescent polymer nanodots as an effective fluorescent sensing platform for label-free detection of Cu(II) ions," *Advanced Materials*, vol. 24, no. 15, pp. 2037–2041, 2012.

[21] F. Y. Wu, S. W. Bae, and J. I. Hong, "A selective fluorescent sensor for Pb(II) in water," *Tetrahedron Letters*, vol. 47, no. 50, pp. 8851–8854, 2006.

[22] K. M. Lee, X. Chen, W. Fang, J. M. Kim, and J. Yoon, "A dual colorimetric and fluorometric sensor for lead ion based on conjugated polydiacetylenes," *Macromolecular Rapid Communications*, vol. 32, no. 6, pp. 497–500, 2011.

[23] X. Peng, J. Du, J. Fan et al., "A selective fluorescent sensor for imaging Cd^{2+} in living cells," *Journal of the American Chemical Society*, vol. 129, no. 6, pp. 1500-1501, 2007.

[24] W. J. Lu, Y. F. Gao, Y. Jiao, S. M. Shuang, C. Z. Li, and C. Dong, "Carbon nano-dots as a fluorescent and colorimetric dual-readout probe for the detection of arginine and Cu^{2+} and its logic gate operation," *Nanoscale*, vol. 9, no. 32, pp. 11545–11552, 2017.

[25] Q. Shu, M. L. Liu, H. Ouyang, and Z. F. Fu, "Label-free fluorescent immunoassay for Cu^{2+} ion detection based on UV degradation of immunocomplex and metal ion chelates," *Nanoscale*, vol. 9, no. 34, pp. 12302–12306, 2017.

[26] Z. Liu, W. He, M. S. Pei, and G. Y. Zhang, "A fluorescent sensor with a detection level of pM for Cd^{2+} and nM for Cu^{2+} based on different mechanisms," *Chemical Communications*, vol. 51, no. 75, pp. 14227–14230, 2015.

[27] Y. L. Huang, A. S. Walker, and E. W. Miller, "A photostable silicon rhodamine platform for optical voltage sensing," *Journal of the American Chemical Society*, vol. 137, no. 33, pp. 10767–10776, 2015.

[28] V. P. Boyarskiy, V. N. Belov, R. Medda, B. Hein, M. Bossi, and S. W. Hell, "Photostable, amino reactive and water-soluble

fluorescent labels based on sulfonated rhodamine with a rigidized xanthene fragment," *Chemistry A European Journal*, vol. 14, no. 6, pp. 1784–1792, 2008.

[29] J. Liu, Y. Q. Sung, H. X. Zhang, H. P. Shi, Y. W. Shi, and W. Guo, "Sulfone-rhodamines: a new class of near-infrared fluorescent dyes for bioimaging," *ACS Applied Materials & Interfaces*, vol. 8, no. 35, pp. 22953–22962, 2016.

[30] P. Hanczyc and L. Sznitko, "Laser-induced population inversion in rhodamine 6G for lysozyme oligomer detection," *Biochemistry*, vol. 56, no. 22, pp. 2762–2765, 2017.

[31] L. Y. Zhang, Q. Zhao, Z. Liang et al., "Synthesis of adenosine functionalized metal immobilized magnetic nanoparticles for highly selective and sensitive enrichment of phosphopeptides," *Chemical Communications*, vol. 48, no. 50, pp. 6274–6276, 2012.

[32] H. Li, Y. H. Shan, L. Z. Qiao, A. Dou, X. Z. Shi, and G. W. Xu, "Facile synthesis of Boronate-decorated Polyethyleneimine-grafted hybrid magnetic nanoparticles for the highly selective enrichment of modified nucleosides and ribosylated metabolites," *Analytical Chemistry*, vol. 85, no. 23, pp. 11585–11592, 2013.

[33] Z. Y. Hu, L. Zhao, H. Y. Zhang, Y. Zhang, R. A. Wu, and H. F. Zou, "The on-bead digestion of protein corona on nanoparticles by trypsin immobilized on the magnetic nanoparticle," *Journal of Chromatography A*, vol. 1334, pp. 55–63, 2014.

[34] Y. Zhang, W. Wang, Q. Li, Q. Yang, Y. Li, and J. Du, "Colorimetric magnetic microspheres as chemosensor for Cu^{2+} prepared from adamantane-modified rhodamine and β-cyclodextrin-modified Fe_3O_4@SiO2 via host–guest interaction," *Talanta*, vol. 141, pp. 33–40, 2015.

[35] Z. Cui, W. Bu, W. Fan et al., "Sensitive imaging and effective capture of Cu^{2+}: towards highly efficient theranostics of Alzheimer's disease," *Biomaterials*, vol. 104, pp. 158–167, 2016.

[36] J. Park, K. An, Y. Hwang et al., "Ultra-large-scale syntheses of monodisperse nanocrystals," *Nature Materials*, vol. 3, no. 12, pp. 891–895, 2004.

[37] X. Meng, Y. Xu, J. Liu, L. Sun, and L. Shi, "A new fluorescent rhodamine B derivative as an "off–on" chemosensor for Cu^{2+} with high selectivity and sensitivity," *Analytical Methods*, vol. 8, no. 5, pp. 1044–1051, 2016.

[38] V. Dujols, F. Ford, and A. W. Czarnik, "A long-wavelength fluorescent chemodosimeter selective for Cu(II) ion in water," *Journal of the American Chemical Society*, vol. 119, no. 31, pp. 7386-7387, 1997.

[39] J. Li, Q. Hu, Y. Zeng, X. Yu, and Z. Pan, "Rhodamine-based fluorescent probes for cations," *Process In Chemistry*, vol. 24, no. 5, pp. 823–833, 2012.

[40] Y. Yuan, M. Tian, F. Feng, S. Meng, and Y. Bai, "Rhodamine-based cations fluorescent probes," *Process In Chemistry*, vol. 22, no. 10, pp. 1929–1939, 2010.

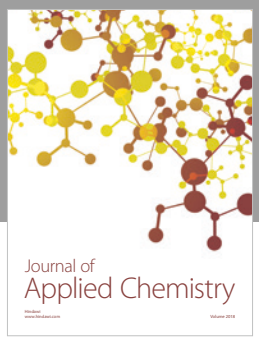

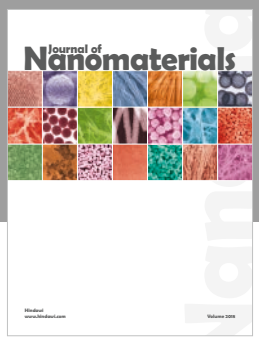

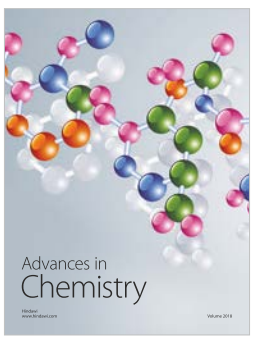
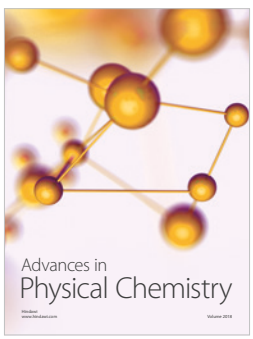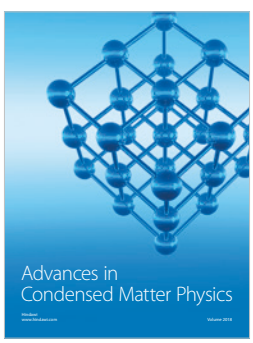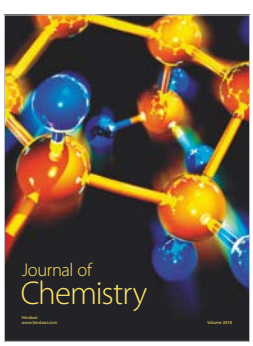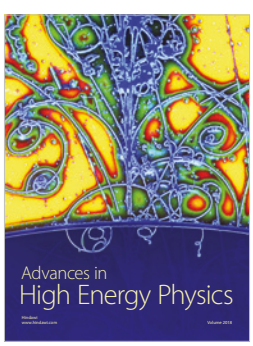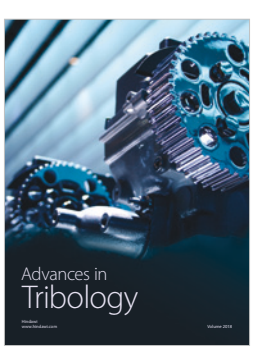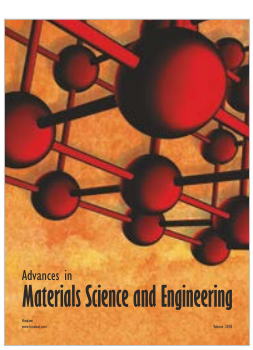
Hindawi
Submit your manuscripts at
www.hindawi.com